Volume 54
Number 41
7 November 2025
Pages 15349-15658

Dalton Transactions

An international journal of inorganic chemistry

rsc.li/dalton

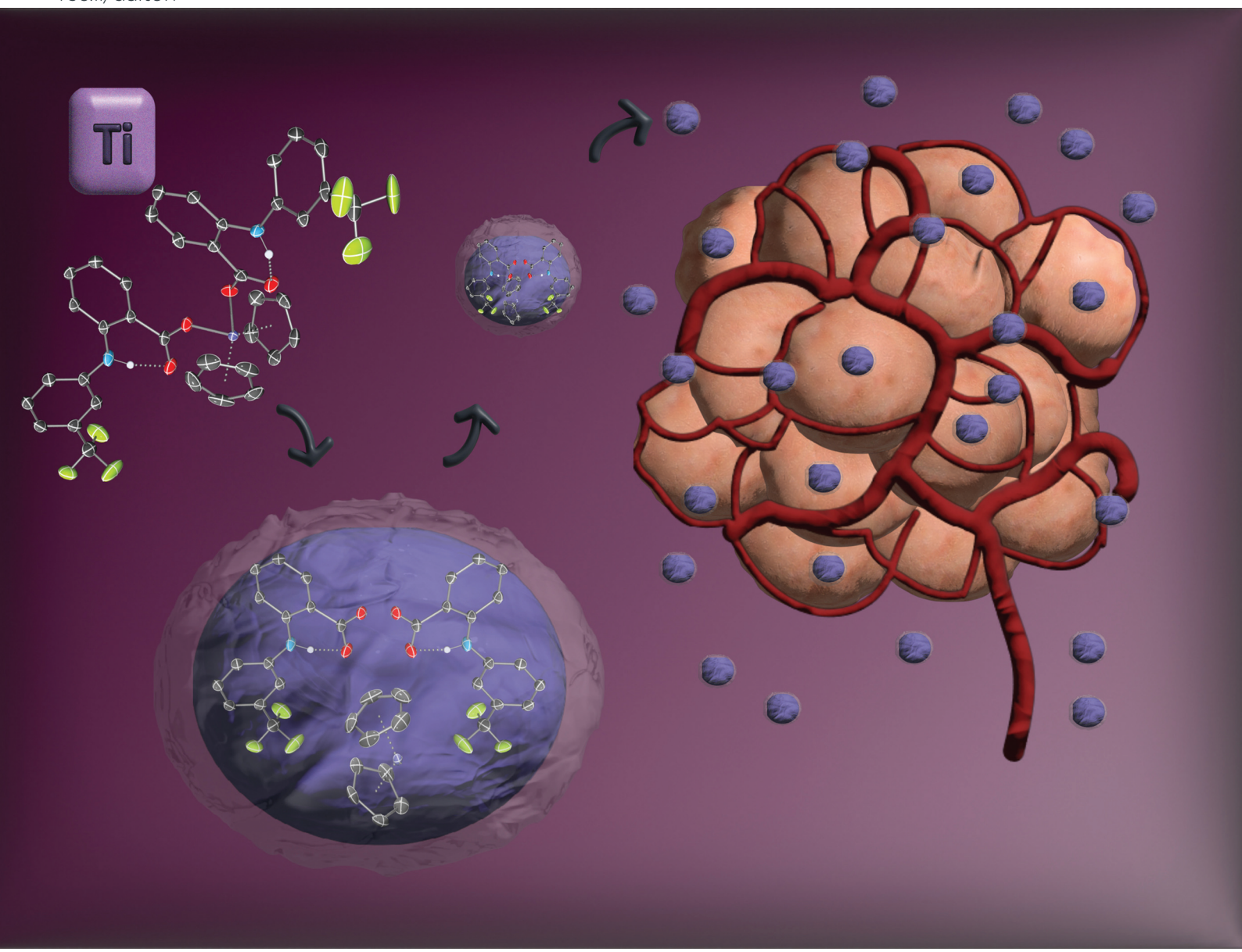

ISSN 1477-9226

ROYAL SOCIETY OF CHEMISTRY

COMMUNICATION

Kogularamanan Suntharalingam, Alexander F. R. Kilpatrick *et al.*

Anti-breast cancer stem cell activity of titanocene complexes of non-steroidal anti-inflammatory drugs

Dalton Transactions

ROYAL SOCIETY OF CHEMISTRY

COMMUNICATION

View Article Online
View Journal | View Issue

Cite this: *Dalton Trans.*, 2025, **54**, 15389

Received 24th June 2025,
Accepted 6th September 2025

DOI: 10.1039/d5dt01491c

rsc.li/dalton

Anti-breast cancer stem cell activity of titanocene complexes of non-steroidal anti-inflammatory drugs

Olympia Mouriki, † Ginevra Passeri, † Karampal Singh, Sarah D. Lamorte, Kuldip Singh, Kogularamanan Suntharalingam * and Alexander F. R. Kilpatrick *

Titanocene(IV)-NSAID complexes $Cp_2Ti(mefenamate)_2$ (4) and $Cp_2Ti(flufenamate)_2$ (5) show enhanced redox stability and potent cytotoxicity against breast cancer stem cells (CSCs), with 5 rivaling salinomycin and cisplatin. Complex 5 induces DNA damage and apoptosis, and its nanoparticle encapsulation improves biocompatibility. This is the first report targeting breast CSCs with titanocene-based metallodrugs.

Titanocene dichloride (Cp_2TiCl_2, **1**) is a Ti(IV) metallocene first reported to exhibit anticancer activity in 1979,[1] demonstrating promising efficacy in mouse tumour models and reduced toxicity relative to cisplatin. However, its clinical development was hindered by poor aqueous stability, rapid hydrolysis, and limited activity in human cells. These drawbacks have motivated efforts to develop substituted titanocene derivatives with improved solubility, stability, and selectivity for cancer cells.[2]

Modifications to both the Cp and X ligands of the Cp_2TiX_2 scaffold have yielded derivatives with enhanced cytotoxicity and pharmacological properties.[3] In particular, replacing chloride with oxygen-donor ligands has improved hydrolytic stability, mirroring strategies used in successful platinum-based drugs.[4] Carboxylate ligands – including κ^2-oxalates and bifunctional linkers – have enabled access to water-soluble, cytotoxic complexes with activity against a range of tumour types.[5] More recently, titanocene-NSAID conjugates have emerged,[6] though their mechanisms of action remain unclear.

Herein we report the synthesis, structural and electrochemical characterisation of two novel bis(κ^1*O*-salicylato) titanocene NSAID complexes. Their cytotoxicity is assessed in breast cancer and breast cancer stem cell (CSC) cultures – an aggressive subpopulation implicated in relapse and metastasis. Nanoparticle encapsulation of the most promising compound is also explored to enhance its safety and therapeutic profile.

Novel titanocene NSAID complexes were prepared *via* a salt metathesis route, by reaction of **1** with the sodium salts of the NSAID carboxylic acids in THF, according to Scheme 1. Complexes $Cp_2Ti(mefenamate)_2$ (**4**) and $Cp_2Ti(flufenamate)_2$ (**5**) were isolated as orange crystalline solids in 79% and 59% yield, respectively (see SI for synthesis and characterisation data).

The identity and solution structure of **4** and **5** were confirmed *via* ^{1}H NMR spectroscopy (Fig. S11 and S13), each revealing one Cp*H* signal with relative integration 10H, and aromatic signals with a total of 14H and 16H, respectively, consistent with bis(salicylate) complexes. Each spectrum shows a downfield singlet resonance (δ = 10.57 (**4**) and 10.86 (**5**) ppm) integrating to 2H assigned to the N*H* environment. ^{13}C NMR spectroscopy data for **4** and **5** (Fig. S12 and S14) are consistent with the proposed structures, with **5** showing a CF_3 carbon quartet at 124.9 ppm ($^1J_{C-F}$ = 272.4 Hz). The ^{19}F NMR spectrum of **5** consists of a single resonance at −62.49 ppm corresponding to the two equivalent CF_3 groups (Fig. S15).

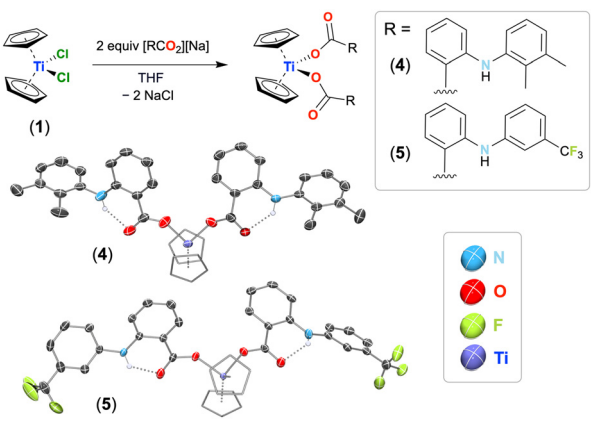

Scheme 1 Synthesis and solid state structures of **4** and **5** with ellipsoids at 50% probability. Selected hydrogen atoms (except H-bonded atoms) are omitted for clarity.

School of Chemistry, University of Leicester, University Road, LE1 7RH Leicester, UK. E-mail: k.suntharalingam@leicester.ac.uk, sandy.kilpatrick@leicester.ac.uk
† These authors contributed equally to this work.

IR spectroscopy of **4** and **5** (Fig. S19 and S20) reveals an intramolecularly bonded N–H stretch (ν = 3227 (**4**) and 3174 (**5**) cm^{-1}), an N–H bend (ν = 1574 (**4**) and 1579 (**5**) cm^{-1}), and a C–O stretch (ν = 1242 (**4**) and 1259 (**5**) cm^{-1}). High resolution mass spectrometry data for **4** and **5** (Fig. S22 and S23) are consistent with the proposed formulations, and bulk purity was confirmed by elemental analysis.

The solid state structures of **4** and **5** were revealed by single crystal X-ray diffraction (Scheme 1) with selected metrical parameters summarised in Table S1 (SI). The Ti centre in each complex shows pseudo-tetrahedral geometry (τ_4 = 0.86), with bond distances and angles similar to those of other structurally characterised titanocene bis(κ^1*O*-carboxylate) complexes.[7] Hydrogen bonding interactions are present between the N–H functionalities on the NSAID ring and the uncoordinated C=O of the κ^1*O*-carboxylate ligands (2.033(6) for **4**; 2.012(13) for **5**), at a longer distance than in the free carboxylic acids (distance 1.888 Å), presumably due to a lower partial negative charge on oxygen as a result of carboxylate binding with Ti. Hydrogen bonding confers co-planarity to the carboxylate and attached aromatic rings within each NSAID ligand, average dihedral angles between CO_2/C_6 mean planes being 16.1(3)° and 1.8(6)° for **4** and **5**, respectively.

The Ti-bound C–O distances (1.286(8) Å for **4**; 1.2942(14) Å for **5**) are long compared to an average C=O double bond (1.24 Å), whereas uncoordinated C–O distances (1.223(8) Å for **4**; 1.231(14) for **5**) are short compared with the average C–O single bond length (1.38–1.42 Å),[8] suggesting a degree of delocalisation across the carboxylate moieties.

The redox properties of **4** and **5** were investigated by cyclic voltammetry in THF/0.2 M [^{n}Bu$_4$N][PF$_6$] at a glassy carbon electrode (Fig. 1, and Table S3). For both complexes, the Ti(IV)/Ti(III) reduction process is not fully reversible, with half-peak potentials, $E_{p/2}$, at −1.46 V (**4**) and −1.38 V (**5**) *vs.* $FeCp_2^{+/0}$. It is postulated that following electrochemical reduction $[Cp_2TiX_2] + e^- \rightleftharpoons [Cp_2TiX_2]^-$ (E_q), the reduced species is unstable with respect to ligand dissociation, $[Cp_2TiX_2]^- \rightarrow [Cp_2TiX] + X^-$ (C_i), under the conditions and timescale of the CV experiment.[9]

Guk *et al.* have recently reported several titanocene(IV) dicarboxylate complexes, and postulated a mechanism of action involving intracellular reduction of Ti(IV) to Ti(II) accompanied by the release of free ligands.[6,7c] However, the redox potentials of some cellular reductants such as NADH, GSH, and ascorbate are approximately −0.72, −0.64, and −0.35 V *vs.* $FeCp_2^{+/0}$ (converted by employing the literature value of $FeCp_2^{+/0}$ = 0.40 V *vs.* NHE in H_2O),[10] respectively. Therefore, the reduction of the metal centre in these complexes from Ti(IV) to lower oxidation states by cellular reductants is not thermodynamically feasible. Hence, we postulate that **4** and **5** remain as Ti(IV) and operate *via* a non-redox pathway, and downstream stability with respect to ligand-dissociation stability and biomolecular interactions of the metal, are not accompanied by a change in oxidation state from Ti(IV). More plausible is the mechanism suggested by Sadler, involving uptake of **1** by transferrin and the hypothesis that this provides a toxic intracellular Ti(IV) species (of unknown structure) that interacts with DNA (and/or RNA).[11]

The potency of the isolated titanocene complexes toward bulk breast cancer cells (HMLER) and breast CSC-enriched cells (HMLER-shEcad) was determined using the colorimetric MTT (3-(4,5-dimethylthiazol-2-yl)-2,5-diphenyltetrazolium bromide) assay. The IC_{50} values associated to the titanocene complexes **1**–**5** were calculated from dose–response curves (Fig. S32–S36) and are presented in Table 1. According to the IC_{50} values, all of the titanocene complexes **1**–**5** displayed micromolar potency towards bulk breast cancer cells and breast CSCs. Titanocene dichloride Cp_2TiCl_2 (**1**) exhibited similar IC_{50} values to the known salicylate-bearing complexes $Cp_2Ti(\kappa^1O\text{-salH})_2$ (**2**) and $Cp_2Ti(\kappa^2O,O'\text{-sal})$ (**3**, Scheme S1),[12] suggesting that incorporation of salicylate onto the titanocene scaffold does not improve potency towards bulk breast cancer cells and breast CSCs. Additionally, the aforementioned result indicates that the differing salicylate chelation modes observed for **2** and **3** does not impact bulk breast cancer cells or breast CSCs potency. Notably, the IC_{50} values for the bis(κ^1*O*-NSAID) titanocene complexes **4** and **5** were significantly ($p < 0.05$, $n = 18$) lower than **1**. This implies that the incorporation of two mefenamate or flufenamate units onto the titanocene scaffold enhances cytotoxicity towards bulk breast cancer cells and breast CSCs. Within the series, **5** displayed

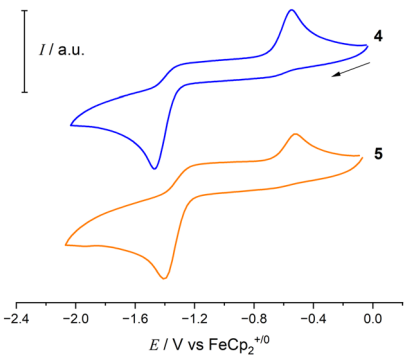

Fig. 1 Stacked CV scans of **4** and **5** in THF/0.2 M [^{n}Bu$_4$N][PF$_6$], scan rate 0.1 V s^{-1}.

Table 1 IC_{50} values of the titanocene complexes **1**–**5**, flufenamic acid, cisplatin, and salinomycin against HMLER and HMLER-shEcad cells and HMLER-shEcad mammospheres determined after 72 h incubation (mean of three independent experiments ± SD)

Complex	HMLER IC_{50} [μM]	HMLER-shEcad IC_{50} [μM]
1	39.52 ± 5.21	46.3 ± 3.61
2	36.50 ± 0.98	53.45 ± 2.36
3	38.25 ± 3.89	40.77 ± 2.42
4	15.54 ± 0.07	32.77 ± 0.98
5	3.90 ± 0.15	4.59 ± 0.10
Flufenamic acid[a]	7.32 ± 1.04	30.86 ± 2.65
Cisplatin[b]	2.57 ± 0.02	5.65 ± 0.30
Salinomycin[b]	11.43 ± 0.42	4.23 ± 0.35

[a] Reported in ref. 13. [b] Reported in ref. 14 and 15.

the greatest potency towards bulk breast cancer cells and breast CSCs.

The IC_{50} value of flufenamic acid towards breast CSCs is 6.7-fold higher than **5**,[13] indicating that complexation of flufenamic acid to the titanocene scaffold improves cytotoxicity towards breast CSCs.

Complex **5** exhibited comparable potency toward bulk breast cancer cells and breast CSC as salinomycin and cisplatin.[14,15] Salinomycin is a polyether antibiotic often used as a positive control for anti-breast CSC cytotoxicity studies,[16] whereas cisplatin is the leading metallodrug used to treat various forms of cancer in the clinic.[4]

To determine whether the cytotoxicity is cancer cell-specific, additional studies were carried out with **5** and non-malignant BEAS-2B (bronchial epithelium) and HEK 293 (embryonic kidney) cells (Fig. S37). Compound **5** was significantly less potent (up to 24-fold, $p < 0.05$, $n = 18$) towards BEAS-2B (IC_{50} value = 93.64 ± 0.19 μM) and HEK 293 (IC_{50} value = 44.40 ± 2.30 μM) cells than HMLER and HMLER-shEcad cells, indicating selectivity for bulk breast cancer cells and breast CSCs over non-cancerous cells.

Stability studies were carried out for **1–5** under conditions relevant to the biological assays. Time course UV-vis spectroscopy of **4** and **5** in cell media : DMSO (200 : 1) showed only gradual spectral changes over 72 h (Fig. S38–S42), with the principal absorption bands retained, indicating that hydrolysis is markedly slower at physiological pH than in coordinating organic solvents. This trend is consistent with our time course NMR studies in THF-d_8/D_2O (Fig. S44–S48) and with the well-documented behaviour of **1**.[17] Complementary mass spectrometry analysis confirmed that all complexes undergo controlled speciation into titanocene-derived oxo/hydroxo species (Fig. S49–S57). These findings suggest that **4** and **5** act as ligand-labile precursors, consistent with the proposed prodrug role for titanocene complexes in Ti(IV) delivery.[11]

Further cell-based studies were carried out with the most effective titanocene complex within the series, Cp_2Ti(flufenamate)$_2$ (**5**) to shed light on its mechanism of action. Cellular uptake and fractionation studies were performed to determine the breast CSC permeability and localisation of **5**. HMLER-shEcad cells treated with **5** (10 μM for 24 h) displayed a significant amount of titanium (82.8 ± 1.3 ng of Ti per million cells), suggestive of effective cell uptake (Fig. S40). Fractionation studies indicated that the vast majority of **5** was actually detected in the membrane fraction suggesting that although **5** is able to enter breast CSCs, a proportion becomes entrapped in the membrane enroute. A smaller, but in the context of DNA-binding anticancer agents, significant amount of titanium was deterred in the nucleus fraction (4.4 ng of Ti/million cells, 6%). This implies that the mechanism of action of **5** could involve biological targets in the nucleus (such as genomic DNA or histones). To provide context, it should be noted that cisplatin is widely accepted to induce its therapeutic effect by damaging DNA and under identical conditions, only 7% is detected in the nucleus of HMLER-shEcad cells.[18] Further, exploring the DNA damaging effects of **5** is plausible as titanocene complexes such as **1** were historically developed and investigated as DNA-binding anticancer agents.[19]

Given that **5** is able to access the breast CSC nucleus, its potential to induce genomic DNA damage and activate the DNA damage response was probed by monitoring the expression of specific biomarkers using immunoblotting methods. HMLER-shEcad cells incubated with **5** (15–60 μM for 24 h) displayed a marked increase in the expression of the phosphorylated forms of H2AX and CHK2, indicative of DNA damage (Fig. S41).

DNA damage, if left unrepaired, can lead to apoptotic cell death.[20] The reorganisation of the cell membrane is an early-stage feature of apoptosis. This involves the translocation of phosphatidylserine residues from the interior to the exterior of the membrane. The cell membrane becomes significantly compromised during late-stage apoptosis. Early-stage apoptosis can be monitored by Annexin V binding to phosphatidylserine residues on the cell exterior, whereas late-stage binding can be detected by the uptake of propidium iodide (an agent that cannot enter health cells).[21] The established dual FITC Annexin V-propidium iodide staining flow cytometry assay was used to determine if **5** evoked apoptosis-like features in breast CSCs. Incubation of **5** (25–100 μM for 48 h) with HMLER-shEcad cells led to a dose-dependent increase in the population of cells expressing early-stage and late-stage apoptotic-like features (Fig. S42). As expected HMLER-shEcad cells treated with cisplatin (25 μM for 48 h) also led to a significant increase in the population of cells expressing early-stage and late-stage apoptotic-like features (Fig. S43). Independent immunoblotting studies were carried out to monitor the caspase-dependent apoptosis pathway. HMLER-shEcad cells treated with **5** (15–60 μM for 24 h) displayed markedly higher levels of cleaved caspase 3, 7, and poly ADP ribose polymerase (PARP) compared to untreated cells (Fig. S41), characteristic of caspase-dependent apoptosis.[22] Taken together the mechanistic studies show that **5** can enter the nucleus of breast CSCs and induce genomic DNA damage, which ultimately leads to caspase-dependent apoptotic cell death. As **5** contains two flufenamate units that are known to modulate cyclooxygenase-2 (COX-2) function, we investigated the ability of **5** to perturb COX-2 expression in breast CSCs. COX-2 is an enzyme that is responsible for converting arachidonic acid into prostaglandins and is implicated in inflammation.[23] Within the CSC context, COX-2 is overexpressed in certain CSCs, plays a role in CSC regulation and maintenance and thus is an established anti-CSC target.[24] HMLER-shEcad cells pre-treated with lipopolysaccharide (LPS) (2.5 μg mL^{-1} for 24 h), to increase basal COX-2 levels, were treated with **5** (10 and 20 μM for 48 h), and the COX-2 expression was determined. COX-2 expression increased significantly upon treatment with **5** (Fig. S44). The observed increase in COX-2 levels could be a downstream genetic response to acute depletion of COX-2 by **5**. To determine if **5** induces COX-2-dependent breast CSC death, cytotoxicity studies were performed with HMLER-shEcad cells pre-treated with prostaglandin E2 (PGE2) (20 μM, 2 h) or LPS

(2.5 μg mL^{-1}, 24 h). The potency of **5** towards HMLER-shEcad cells decreased significantly under both conditions (IC_{50} value = 12.10 ± 0.99 μM with PGE2 and IC_{50} value = 16.60 ± 1.10 μM with LPS, $p < 0.05$) (Fig. S45). Collectively, the flow cytometric and cytotoxicity studies suggest that the mechanism of action of **5** could be related to COX-2 modulation.

With the aim of enhancing the safety profile of **5** the complex was encapsulated into PEG-PLGA (5000 : 30 000 Da, 1 : 1 LA : GA) nanoparticles. PEG-PLGA copolymers form sphere-like nanoparticles in aqueous solutions (with a hydrophobic PLGA inner core and a hydrophilic PEG outer layer) due to their amphiphilic nature. PEG-PLGA nanoparticles (**5 NP**) were prepared with a 10% feed of **5** using the nanoprecipitation method. The loading and encapsulation efficiency of **5** into **5 NP**, calculated by measuring the titanium concentration using ICP-MS, was 0.46% and 4.55%, respectively. These values are consistent with those obtained for the encapsulation of other metal complexes into PEG-PLGA-based nanoparticles.[15]

According to dynamic light scattering (DLS) studies the average nanoparticle diameter of **5 NP** was 129.7 ± 0.61 nm and the polydispersity was 0.099 ± 0.007 (Fig. 2A). The morphology of **5 NP** was assessed by transmission electron microscopy (TEM). The TEM images confirmed that **5 NP** form relatively uniform spherical structures with an average size of 95.76 ± 37.41 nm (Fig. 2B). The average nanoparticle diameter determined by DLS and TEM are in reasonable agreement.

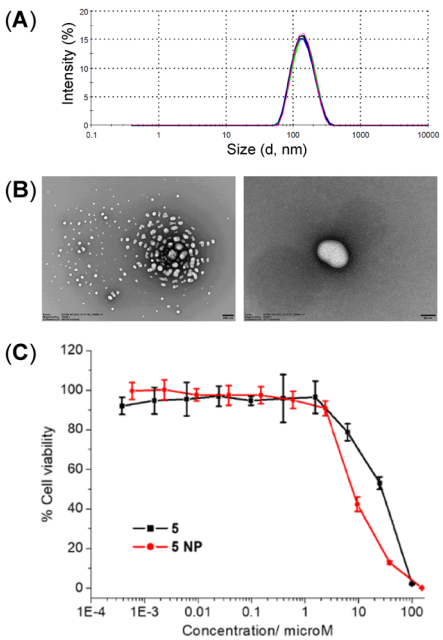

Fig. 2 (A) Dynamic light scattering size distribution of **5 NP** suspended in water. Size refers to diameter of nanoparticles in nm. (B) TEM images of **5 NP** suspended in water at ×15 000 magnification, scale bar = 200 nm and ×80 000 magnification, scale bar = 50 nm. (C) Representative dose–response curves for the treatment of HMLER-shEcad cell with **5 NP** or the payload 5.

The potency of the nanoparticle formulation **5 NP** towards breast CSC-enriched HMLER-shEcad cells was determined using the MTT assay, and the IC_{50} value was calculated from the corresponding dose–response curve (Fig. 2C). The nanoparticle formulation **5 NP** displayed an IC_{50} value of 7.70 ± 0.21 μM, slightly higher than that observed for the payload **5**. This shows that encapsulation of **5** into PEG-PLGA (5000 : 30 000 Da, 1 : 1 LA : GA) nanoparticles improves the safety profile of **5**. This is consistent with previous reports that show polymeric nanoparticles reduce the toxicities of incorporated compounds.[25]

Conclusions

In conclusion we report the synthesis and extensive characterisation of titanocene(IV) complexes bearing NSAID ligands. Single-crystal X-ray diffraction of $Cp_2Ti(mefenamate)_2$ (**4**) and $Cp_2Ti(flufenamate)_2$ (**5**) confirms pseudo-tetrahedral geometries, with two Cp ligands and two monodentate NSAID moieties bound to a Ti centre. Titanocene cytotoxicity is widely linked to hydrolytic activation, and our electrochemical data and stability studies clarify that this likely involves ligand dissociation and hydrolysis – not formal Ti(IV)/Ti(III) redox processes.

Biological evaluation revealed micromolar cytotoxicity for all titanocene compounds (**1–5**) against breast cancer cells and cancer stem cells (CSCs). Notably, bis(NSAID) derivatives **4** and **5** showed significantly improved potency over Cp_2TiCl_2 (**1**), highlighting the benefit of flufenamate and mefenamate ligation. Furthermore, encapsulation of **5** in PEG-PLGA nanoparticles reduced its toxicity, suggesting improved safety and delivery potential.

This is the first study to investigate titanocene complexes in the context of anti-breast CSC therapy. These results demonstrate the potential of Ti(IV) compounds as promising leads for CSC-targeted chemotherapy and encourage broader exploration of metal-NSAID frameworks in anticancer drug design.

Author contributions

Methodology, validation, formal analysis, investigation, Olympia Mouriki, Ginevra Passeri, Karampal Singh, Sarah D. Lamorte, Kuldip Singh, Kogularamanan Suntharalingam, Alexander F. R. Kilpatrick; conceptualisation, writing – original draft, writing – review & editing, funding acquisition, supervision and project administration Kogularamanan Suntharalingam, Alexander F. R. Kilpatrick.

Conflicts of interest

There are no conflicts to declare.

Data availability

Supplementary information: general experimental procedures and instrumentation, synthesis and characterisation data, NMR, IR and mass spectra, additional X-ray crytallographic and cyclic voltammetry data, cytotoxicity data, time course UV-vis spectroscopy, NMR spectroscopy and mass spectrometry stability studies, and mechanism of action studies. See DOI: **https://doi.org/10.1039/d5dt01491c**.

CCDC 2373016–2373018 (**2**, **4**, and **5**) contain the supplementary crystallographic data for this paper.[26a–c]

The raw data for all the figures are openly available on Figshare: **https://doi.org/10.25392/leicester.data.29665502**.

Acknowledgements

We thank the Engineering and Physical Sciences Research Council (EPSRC) for the award of an Early Career Researcher International Collaboration Grant (EP/Y002695/1, A. F. R. K.). We are grateful to the NMR Facility in the School of Chemistry at the University of Leicester supported by the EPSRC (EP/W02151X/1) and Dr Rebecca R. Hawker and Dr Adam Khan for assistance with non-routine NMR measurements. X-ray diffraction at the University of Leicester was supported by the EPSRC (EP/V034766/1). Summer placement students Eisha Abbas, Aliyah Bham, Kieran Findley-Patel, Harsh Sagar from In2ScienceUK are acknowledged for help with repeat synthesis of the literature titanocene compounds described herein.

References

1 H. Köpf and P. Köpf-Maier, *Angew. Chem., Int. Ed. Engl.*, 1979, **18**, 477–478.
2 M. Cini, T. D. Bradshaw and S. Woodward, *Chem. Soc. Rev.*, 2017, **46**, 1040–1051.
3 (*a*) O. R. Allen, L. Croll, A. L. Gott, R. J. Knox and P. C. McGowan, *Organometallics*, 2004, **23**, 288–292; (*b*) O. R. Allen, A. L. Gott, J. A. Hartley, J. M. Hartley, R. J. Knox and P. C. McGowan, *Dalton Trans.*, 2007, **36**, 5082–5090; (*c*) G. D. Potter, M. C. Baird and S. P. C. Cole, *J. Organomet. Chem.*, 2007, **692**, 3508–3518.
4 T. C. Johnstone, K. Suntharalingam and S. J. Lippard, *Chem. Rev.*, 2016, **116**, 3436–3486.
5 (*a*) J. Claffey, M. Hogan, H. Müller-Bunz, C. Pampillón and M. Tacke, *ChemMedChem*, 2008, **3**, 729–731; (*b*) J. Ceballos-Torres, M. J. Caballero-Rodríguez, S. Prashar, R. Paschke, D. Steinborn, G. N. Kaluerović and S. Gómez-Ruiz, *J. Organomet. Chem.*, 2012, **716**, 201–207; (*c*) Y. F. Mui, J. Fernández-Gallardo, B. T. Elie, A. Gubran, I. Maluenda, M. Sanaú, O. Navarro and M. Contel, *Organometallics*, 2016, **35**, 1218–1227; (*d*) J. Fernández-Gallardo, B. T. Elie, T. Sadhukha, S. Prabha, M. Sanaú, S. A. Rotenberg, J. W. Ramos and M. Contel, *Chem. Sci.*, 2015, **6**, 5269–5283.
6 D. A. Guk, K. R. Gibadullina, A. A. Moiseeva, Y. K. Grishin, V. A. Roznyatovsky, D. S. Prosuntsova, I. A. Ananieva, E. R. Gandalipov, A. A. Shtil and E. K. Beloglazkina, *New J. Chem.*, 2023, **48**, 1650–1660.
7 (*a*) W. Scherer, P. Meixner, K. Batke, J. E. Barquera-Lozada, K. Ruhland, A. Fischer, G. Eickerling and K. Eichele, *Angew. Chem., Int. Ed.*, 2016, **55**, 11673–11677; (*b*) T. S. Basu Baul, R. Manne and E. R. T. Tiekink, *Inorg. Chim. Acta*, 2019, **484**, 469–480; (*c*) D. A. Guk, K. R. Gibadullina, R. O. Burlutskiy, K. G. Pavlov, A. A. Moiseeva, V. A. Tafeenko, K. A. Lyssenko, E. R. Gandalipov, A. A. Shtil and E. K. Beloglazkina, *Int. J. Mol. Sci.*, 2023, **24**, 3340.
8 (*a*) P. Pyykkö and M. Atsumi, *Chem. – Eur. J.*, 2009, **15**, 186–197; (*b*) P. Pyykkö and M. Atsumi, *Chem. – Eur. J.*, 2009, **15**, 12770–12779.
9 (*a*) R. Meunier-Prest, G. Lamblin, A. Mailfert and S. Raveau, *J. Electroanal. Chem.*, 2003, **541**, 175–183; (*b*) T. Hilche, S. L. Younas, A. Gansäuer and J. Streuff, *ChemCatChem*, 2022, **14**, e202200530.
10 (*a*) I. H. Segel, *Biochemical calculations: how to solve mathematical problems in general biochemistry*, Wiley, 1991; (*b*) W. Scherer, P. Meixner, K. Batke, J. E. Barquera-Lozada, K. Ruhland, A. Fischer, G. Eickerling and K. Eichele, *Angew. Chem., Int. Ed.*, 2016, **55**, 11673–11677; (*c*) E. G. Ball, *J. Biol. Chem.*, 1937, **118**, 219–239; (*d*) N. G. Connelly and W. E. Geiger, *Chem. Rev.*, 1996, **96**, 877–910.
11 A. M. Pizarro, A. Habtemariam and P. J. Sadler, in *Medicinal Organometallic Chemistry*, ed. G. Jaouen and N. Metzler-Nolte, Springer, Berlin, Heidelberg, 2010, pp. 21–56.
12 (*a*) Z.-Q. Hang, S.-W. Lu, H.-F. G. Dalian, Z.-R. Lu and Y.-K. Zhou, *Synth. React. Inorg. Met.-Org. Chem.*, 1992, **22**, 883–892; Y. Wu, C. Chen, G. Jia, X. Zhu, H. Sun, G. Zhang, W. Zhang and Z. Gao, *Chem. – Eur. J.*, 2014, **20**, 8530–8535; (*b*) Z. Zeng, *Synth. React. Inorg. Met.-Org. Chem.*, 2001, **31**, 1285–1296; (*c*) J.-L. Li, Z.-W. Gao, P. Sun, L.-X. Gao and W. Tikkanen, *Inorg. Chim. Acta*, 2011, **368**, 231–236; (*d*) Z. Gao, D. Hu, L. Gao, X. Zhang, Z.-T. Zhang and Q. Liang, *J. Organomet. Chem.*, 2001, **629**, 47–53.
13 J. Fang, O. N. Orobator, C. Olelewe, G. Passeri, K. Singh, S. G. Awuah and K. Suntharalingam, *Angew. Chem., Int. Ed.*, 2024, **63**, e202317940.
14 J. N. Boodram, I. J. Mcgregor, P. M. Bruno, P. B. Cressey, M. T. Hemann and K. Suntharalingam, *Angew. Chem., Int. Ed.*, 2016, **55**, 2845–2850.
15 A. Eskandari and K. Suntharalingam, *Chem. Sci.*, 2019, **10**, 7792–7800.
16 P. B. Gupta, T. T. Onder, G. Jiang, K. Tao, C. Kuperwasser, R. A. Weinberg and E. S. Lander, *Cell*, 2009, **138**, 645–659.
17 (*a*) J. H. Toney and T. J. Marks, *J. Am. Chem. Soc.*, 1985, **107**, 947–953; (*b*) X. Chen and L. Zhou, *J. Mol. Struct.: THEOCHEM*, 2010, **940**, 45–49; (*c*) U. Olszewski and G. Hamilton, *Anti-Cancer Agents Med. Chem.*, 2010, **10**, 302–311.
18 A. Eskandari, A. Kundu, S. Ghosh and K. Suntharalingam, *Angew. Chem., Int. Ed.*, 2019, **58**, 12059–12064.

19 S. Burma, B. P. Chen, M. Murphy, A. Kurimasa and D. J. Chen, *J. Biol. Chem.*, 2001, **276**, 42462–42467.
20 W. P. Roos, A. D. Thomas and B. Kaina, *Nat. Rev. Cancer*, 2016, **16**, 20–33.
21 I. Vermes, C. Haanen, H. Steffens-Nakken and C. Reutellingsperger, *J. Immunol. Methods*, 1995, **184**, 39–51.
22 G. M. Cohen, *Biochem. J.*, 1997, **326**, 1–16.
23 M. E. Turini and R. N. DuBois, *Annu. Rev. Med.*, 2002, **53**, 35–57.
24 L. Y. Pang, E. A. Hurst and D. J. Argyle, *Stem Cells Int.*, 2016, **2016**, 2048731.
25 (*a*) W. H. De Jong and P. J. A. Borm, *Int. J. Nanomed.*, 2008, **3**, 133–149; (*b*) A. Eskandari, J. N. Boodram, P. B. Cressey, C. Lu, P. M. Bruno, M. T. Hemann and K. Suntharalingam, *Dalton Trans.*, 2016, **45**, 17867–17873.
26 (*a*) O. Mouriki, G. Passeri, K. Singh, S. D. Lamorte, K. Singh, K. Suntharalingam and A. F. R. Kilpatrick, CCDC 2373016: Experimental Crystal Structure Determination, 2025, DOI: **10.5517/ccdc.csd.cc2kn9xg**; (*b*) O. Mouriki, G. Passeri, K. Singh, S. D. Lamorte, K. Singh, K. Suntharalingam and A. F. R. Kilpatrick, CCDC 2373017: Experimental Crystal Structure Determination, 2025, DOI: **10.5517/ccdc.csd.cc2kn9yh**; (*c*) O. Mouriki, G. Passeri, K. Singh, S. D. Lamorte, K. Singh, K. Suntharalingam and A. F. R. Kilpatrick, CCDC 2373018: Experimental Crystal Structure Determination, 2025, DOI: **10.5517/ccdc.csd.cc2kn9zj**.